Brage IMR –

Havforskningsinstituttets institusjonelle arkiv

Brage IMR –

Institutional repository of the Institute of Marine Research

Foto: Leif Nøttestad

Short-term hydrographic variability in a stratified Arctic fjord

J. Skarðhamar[1]* & H. Svendsen[2]

[1] University of Tromsø, N-9037 Tromsø, Norway
[2] Geophysical Institute, University of Bergen, N-5007 Bergen, Norway
* Corresponding author (e-mail: jofrid.skardhamar@uit.no)

Number of words of text: 3496
References: 24
Tables: 2
Figures: 6

Abbreviated title: **Arctic fjord hydrographic variability**

Abstract

Fjords in the Arctic often have a more complex circulation pattern than the classical two-dimentional estuarine circulation. This is due to the effects of the Earth's rotation on stratified waters in wide fjords. Observations from a semi-enclosed fjord basin, Van Mijenfjorden on Spitsbergen, show that the hydrography and circulation vary considerably on short time scales (hours) in the summer season. The depth and distribution of the low salinity upper water layer respond quickly to changes in the wind field. The Coriolis effect has an essential impact on the circulation, inducing eddy-like flow patterns, and strong cross-fjord gradients. Within the upper layer, the lowest salinity values and highest temperatures were found on the northern side of the fjord in calm wind periods. When the wind was strong from west the cross-fjord gradients were reversed. Internal wave activity contributes to large vertical displacement of water below the upper layer. Knowledge of such strongly variable hydrographic conditions in fjords are important for sampling strategy and interpretation of data, for instance of primary production and sedimentation processes, and for the understanding of fjords as depositional systems.

Sill fjords normally have distinct vertical stratification with an approximate three-layer structure; an upper layer with low salinity above a more saline intermediate layer, and high salinity basin water below the sill depth. Large seasonal variations in air temperature and freshwater discharge lead to significant variations in both the stratification and circulation pattern. In Arctic fjords, the described stratification structure appears only in the summer season (see e.g. Svendsen *et al*. 2002), while in winter the water masses are overturned due to cooling. In general the circulation in fjords is forced by a combination of external forces, such as wind, freshwater discharge and tides. The motions are modified by topography and friction, and in wide stratified fjords rotational dynamics (Coriolis effect) may have an important impact on the fjord dynamics. The effect of the Coriolis force depends on the stratification, and therefore the impact of the earth rotation will vary both seasonally and locally within a fjord. For details about physical processes in fjords, see e.g. Farmer & Freeland (1983) and Svendsen (1986).

The physical oceanography of most fjords on Spitsbergen is poorly investigated. Marine biological and geological investigations have been carried out in Van Mijenfjorden and several other fjords in the area, but contemporary studies of the physics of the fjords have often been limited to a few CTD stations, which is insufficient to give information about complex circulation and exchange patterns. Three exceptions are the fjords Kongsfjorden, Isfjorden and Hornsund which have been subjects to several oceanographic research projects during the last decade (e.g. Ingvaldsen *et al*. 2001, Svendsen *et al*. 2002, Cottier *et al.* 2005, Nilsen *et al*. 2008, Tverberg & Nøst 2009). Van Mijenfjorden differs from the other Spitsbergen fjords by its mouth being nearly closed by an island, restricting the water exchange between the fjord basin and coastal water masses. This fjord is therefore a good “laboratory” fjord for process studies, see e.g. Widell *et al*. (2006) and Fer & Widell (2007) who studied turbulence due to ice freezing. The present work focuses on the effects of wind and the short-term variability of the fjord circulation and hydrography. The investigation was based on field data from a summer season, i.e. without ice cover. The semi-enclosed nature of Van Mijenfjorden makes wind effects pronounced and easily distinguishable relative to fjord-ocean exchange processes. However, the wind effects described here are relevant for other arctic and sub-arctic fjords as well.

Materials and methods

Study area

Van Mijenfjorden is a 50 km long sill fjord at the west coast of Spitsbergen (Figure 1). The mean width of the fjord is 10 km, and the surface area covers 515 km^2 (Schei *et al*. 1979). The island Akseløya lies across the mouth of the fjord, leaving two narrow sounds where the water exchange between the fjord and coast takes place. The sound Akselsundet, on the northern side of Akseløya, is 1 km wide with sill depth of 34 m (Fer & Widell 2007). The sound on the southern side, Mariasundet, is intersected by a small islet, leaving a 600 m wide and 2 m deep passage to the north of the islet, and a 500 m wide and 12 m deep passage to the south. The majority of the water exchange takes place through Akselsundet, where the tidal currents are strong with current speed up to 3 m s^{-1} (Norwegian hydrographic service, 1990). Tidal choking (Stigebrandt 1980) can create tidal jets through the sounds during flood and is an important driving force for the mean circulation in the fjord (Bergh 2004).

Van Mijenfjorden consists of two basins. The outer basin is 115 m deep and is separated from the 74 m deep inner basin by a 45 m deep sill, which is the remains of the moraine after the major surge of the glacier Paulabreen 600-250 years ago (Rowan *et al*. 1982; Hald *et al.* 2001). Van Mijenfjorden is surrounded by tall mountains (800-1200 m) and broad valleys, including one of the largest ice-free valleys on Svalbard, Reindalen. Two glaciers calve in the fjord; Fridtjovbreen in Fridtjovhavna near the fjord mouth and Akselsundet, and Paulabreen in Rindersbukta at the head of the fjord.

Observations of wind at Svea in the inner part of the fjord show that the prevailing winds are from northeast, i.e. katabatic down-fjord wind, except in the summer season when up-fjord winds occur nearly as frequent as down-fjord winds (Hanssen-Bauer *et al*. 1990). The climate of west Spitsbergen is relatively dry. The total precipitation varies between 180 and 440 mm a year (Hanssen-Bauer *et al*. 1990), with minimum in April-June and maxima in August, February and March.

The fjords of west Spitsbergen are normally covered by ice from December to May/June. Van Mijenfjorden is ice covered for a longer period than the other fjords, because of the protecting effects of Akseløya. Some years the fjord freezes up as early as in September, and the fjord is normally not navigable by boat until the beginning of June (Norwegian hydrographic service, 1990). Little drift ice enters the fjord, so the fjord ice mainly consists of locally frozen fjord water and ice from the glaciers. The sounds Akselsundet and Mariasundet are ice free all winter due to the strong tidal currents.

Field data

The field data were collected during a cruise with R/V Håkon Mosby in the period from 28 July to 3 August 1996. Repeated hydrographic mapping of Van Mijenfjorden was performed with a SeaBird CTD covering a dense station net of 23 stations (Figure 1) three times: 28 July, 31 July and 2 August. One of the CTD stations was repeated every hour 22 times from 31 July to 1 August. The CTD was calibrated at the Institute of Marine Research, Bergen, in accordance with the ICES procedure prior to the cruise. The data were averaged over depth intervals of 2 m.

Current measurements were obtained using Aanderaa current meters RCM4 and RCM7 deployed on three moorings; see Figure 1 and Table 1 for positions and depths. The moorings were deployed for a period of 6 days. The measuring interval was 10 minutes, and the measurements were averaged over a 40-hours Butterworth low-pass filter to remove the tidal effects (see e.g. Emery & Thomson 1997).

An automatic weather station was installed on the innermost mooring, measuring wind speed and wind direction. In addition, wind speed, wind direction and air temperature were recorded from the weather station on board the ship at every CTD station. Meteorological data were also available from the Norwegian Meteorological Institute’s weather station at Svea.

Results

Hydrography

The vertical salinity and temperature distribution revealed a stably stratified fjord with strong vertical salinity and temperature gradients in the upper 10-15 m (Figure 2). Below this, the salinity increased more slowly with depth, from 32 just below the pycnocline to 34 at 80 m in the outer basin, and 50 m in the inner basin (Figure 2a). The temperature decreased from 1 ºC just below the pycnocline to -1 ºC at 80-90 m in the outer basin, and at 50 m in the inner basin (Figure 2b). The vertical thickness and horizontal distribution of the low salinity layer (salinity < 31) varied considerably between the three surveys and between the inner and outer basin. The low salinity layer had a more even distribution along the longitudinal axis of the fjord during the first and last surveys than during the second survey. During the second survey the pycnocline depth was shallower in the outer basin (Figure 3, lower panels) and deeper in the inner basin compared to the other two surveys (Figure 3, upper panels). Also the horizontal across-fjord gradients of salinity and temperature varied during the field campaign. In general, higher temperatures and lower salinities were measured on the northern side of the fjord compared to the southern side on the first and third survey, with horizontal salinity gradients between 0.4 and 0.7 km^{-1} at 4 m depth in the main basin On the second survey, the gradients were reversed with the lowest salinities and highest temperatures along the southern side of the fjord (Figure 4), and horizontal salinity gradients between -0.3 and -0.5 km^{-1}.

The data from the time series station show large vertical excursion of water properties below the pycnocline. Within four hours, the isoline for salinity 33 ascends from 35 m depth to 15 m depth, before abruptly sinking back down again (Figure 5).

Currents

The current meter measurements showed strongest current speed near the surface (measured at 2 m depth) and weakest current speeds at depth 60-70 m at all three moorings (Figure 6). Variable current directions were recorded at all depths at the inner mooring (Figure 6a). On the northern side of the fjord, the currents were directed out of the fjord at all depths almost throughout the period (Figure 6b). On the southern side of the fjord the current direction varied between in to and out of the fjord at 2 m depth, and also 70 m depth, while the currents were constantly directed inwards at depths 10 m and 30 m (Figure 6c).

Meteorological observations

The air temperature varied between 3.5 ºC and 6 ºC during the cruise. The wind was blowing with a westerly component, i.e. towards the head of the fjord, the whole cruise period (Figure 6a), and the wind speed varied between 0.3 m s^{-1} (calm) and 12 m s^{-1}. Weak wind was recorded the first days of the cruise, with wind speed less than 5 m s^{-1} the first day (28 July) followed by one day of calm wind (29 July). The wind speed increased to 6-10 m s^{-1} in the afternoon 30 July, lasting for two days before dropping to less than 5 m s^{-1} 1-2 August. The mean wind speeds and directions for the three CTD-surveys are given in table 2.

Discussion

The observed horizontal salinity and temperature gradients, and their variability, within the fjord can be explained by three main factors; the positions of the largest river mouths, the Coriolis effect and wind. Two large valleys have outlets to the northern side of the fjord, and supply large volumes of freshwater on that side of the fjord. In addition, freshwater from Fridthjovbreen is discharged on the northern side, near the fjord mouth. The valleys on the southern side of the fjord are smaller and probably have less freshwater discharge. This alone could explain the lower salinity on the northern side of the fjord during calm wind conditions.

The dynamic effect of the Earth's rotation on fjords depends on the width of the fjord and the vertical stratification (see e.g. Cushman-Roisin *et al*. 1994). If we regard Van Mijenfjorden as a two-layer system with a 7 m thick upper layer of water density 1020 kg m^{-3}, and 80 m thick deep layer of density 1026 kg m^{-3} (based on the present field measurements from the outer basin), the baroclinic Rossby radius is 4.3 km. This radius is less than half of the fjord width in the outer basin, and consequently the motions here are strongly affected by the Earth's rotation. Similar considerations for the inner basin, with a 10 m thick upper layer of water density 1019 kg m^{-3} and a 40 m thick deep layer of density 1026 kg m^{-3} (measurements from the inner basin), give a Rossby radius of 5.2 km, which corresponds to the fjord width in this area. Thus, the Coriolis force affects the circulation also in the inner basin, however, to a lesser degree than the outer part of the fjord. The Earth's rotation acts to deflect the outward flowing surface current containing low-salinity water, to the right, thus following the northern shore towards the mouth. Consequently, the river water discharged on the northern side of the fjord will not spread evenly over the fjord's surface, but be guided along the northern coast towards the fjord's mouth. This effect contributes to maintain a salinity gradient across the fjord, with the lowest salinities on the northern side of the fjord, as observed.

Wind driven Ekman transport will also affect the surface salinity and temperature distribution. Easterly winds amplify the estuarine circulation with the out-flowing low-salinity water along the northern side of the fjord, while westerly wind may counteract this circulation. The fjord was surveyed with CTD measurements three times during the cruise. During the first and third survey the wind was weak, with mean wind speed 1 m s^{-1} (table 2), while stronger westerly wind (7 m s^{-1}) was blowing during the second survey. The different wind conditions were clearly reflected in the horizontal temperature and salinity gradients across the fjord. The day of the strongest westerly (up-fjord) winds (31 July), the surface salinity and temperature gradients across the fjord were reversed compared to the other two surveys. The stratification was reduced, and the horizontal gradients were evident to larger depths when the wind was strong, indicating deeper vertical mixing. The up-fjord wind forces the “warm” and low-salinity surface water to the south and upwelling of colder and more saline water reaches the surface along the northern side of the fjord. This fjord response is in accordance with the theory of estuarine circulation in broad fjords of Cushman-Roisin *et al.* (1994).

The current meter data and wind measurements from the innermost mooring show a relationship between westerly winds and current direction towards east (up-fjord) at all depths. The near-surface current turned 180º when the wind ceased, driven by a down-fjord pressure gradient established during the period of strong up-fjord wind pushing water to the fjord head. The near-surface current direction at the southernmost mooring varied similarly with the wind direction at depth 2 m. The other current meters did not reveal such clear relationships with changing wind. Thus, the circulation in the fjord is a complex result of combined effects of estuarine circulation, rotational dynamics and wind effects.

Our time series are too short to detect long period internal waves, such as Kelvin waves. However, we have observed large vertical displacement of water masses within the deeper layer, indicating internal wave activity in the fjord. The Ekman transport and piling up of water against the southern shore during up-fjord winds and against the northern shore during down-fjord winds causes, as described above, disturbances of the upper layer thickness. Theoretically, the distortion of the interface may travel as a Kelvin wave with the shore on the right hand side, looking in the direction of its propagation (Asplin 1995; Svendsen 1995). The mixed water in the narrow entrances to the fjord would prevent Kelvin waves from leaving the fjord, instead such waves can be guided along the shore around the whole basin. The combined effect of surface elevation and interface displacement could lead to quasi-geostrophically balanced steady state currents circulating the basin (Asplin 1995). Given the varying wind pattern, and since the currents will persist for some time after a wind event, the flow field at any given time may be related to a superposition of several Kelvin waves circulating the fjord. In order to discuss the influence of the tide on the flow field in the fjord it is appropriate to estimate the internal Froude number (F_i) for the topographic constriction Akselsundet, $F_i=u/c$, where u is the velocity of the upper layer, and c is the phase speed of a long internal wave on the interface between the layers; ($c = \sqrt{g' h}$), where g' is the reduced gravity and h is the depth of the upper layer. Using the same two-layer structure as described above, the phase speed of the wave is estimated to 0.6 m s^{-1}. Current velocity of the order 2 m s^{-1} in the sound (as measured by Bergh 2004) and the phase speed calculated above yields $F_i>>1$, i.e. supercritical conditions. Supercritical conditions imply that kinetic energy exceeds the potential energy of the field, thus inhibiting the development of wave-like behaviour on the interface. However, the speed of the tidal current varies considerably during the tidal period. Internal flows that are sub-critical may therefore readily occur during a tidal period which then makes the conditions favourable for internal tides to be generated, and appear as “pulses” travelling in the same direction as the Kelvin waves. Inall *et al.* (2005) found that approximately 1/3 of the barotropic tidal energy in a sill fjord with supercritical conditions was transformed to internal wave energy. Model simulations by Støylen & Weber (accepted) showed that internal Kelvin waves, generated by barotropic tidal pumping in the sounds, can propagate cyclonically around the basin of Van Mijenfjorden, and they argue that the associated drift can contribute significantly to the horizontal circulation in the fjord.

The shallow and narrow sounds at the fjord's mouth and the sill between the two fjord basins prevent free water mass exchange between Bellsund and the fjord, and between the two fjord basins. As a consequence, the local freshwater discharge to the fjord strongly affects the salinity distribution within the fjord area in the melting season, when the salinity in the upper layer is markedly lower than that measured in Bellsund. The high salinity and low temperature of the deep water is probably caused by sinking of dense surface water (vertical convection) formed by cooling and brine release during ice freezing in winter. An alternative source of deep water renewing is intrusion of coastal water from Bellsund. However, since the temperature of the deep water was lower than that measured in Bellsund in summer, a possible renewal of the deep water caused by intrusion, must have taken place during the preceding winter. The surface water temperatures in the fjord were higher than those measured in Bellsund during our surveys. In addition to direct solar heating of the surface layer, the high temperature can be explained by supply of "warm" river water that has been warmed up in the shallow river beds and tidal flats on its way to the fjord. Weslawski *et al*. (1991) measured temperatures up to 14 ºC in shallow waters over dark sediments in Vestervågen, Bellsund.

Summary and conclusion

Van Mijenfjorden is characterized by short-time variations in current pattern and the horizontal and vertical distribution of temperature and salinity. Wind and the Earth's rotation (Coriolis effect) are the dominating factors determining the pattern and strength of the circulation in the fjord in summer, when a low salinity upper layer is present in the fjord. The major part of the fjord is dominated by a prevailing eddy-like flow pattern, which was reversed several times during our cruise period, related to varying wind strength and direction. Up-fjord westerly wind forces the "warm" and low-salinity surface water to the south, and upwelling of colder and more saline water reaches the surface along the northern side of the fjord. In periods of calm wind, and probably also of down-fjord wind, the lowest salinity water is found along the northern side of the fjord. The alternating circulation, the corresponding changing of cross- and along-fjord gradients in salinity and temperature, and the excitation of internal waves, entail that the fjord is subject to high frequency variations of the hydrographic conditions in time and space. It is of importance for researchers from all disciplines sampling in fjords to be aware of such strongly variable conditions to be able to interpret their data. In wide fjords the expected main transport pathway of sediment-rich surface water of terrestrial origin is along the right hand side of the fjord (i.e. following the northern shore for Van Mijenfjorden), due to the Coriolis effect. It is therefore reasonable to assume the highest sedimentation rate on that side of the fjord. We have shown here that strong up-fjord winds can disturb this pattern, by deflecting the brackish water plume towards the opposite shore, thus reversing the cross-fjord hydrographic gradients. Sedimentation is thus expected to take place on both sides of wide fjords, but with cross-fjord differences in sedimentation rates being likely, depending on the wind conditions in the fjord.

Reference list

Asplin, L. 1995. Examination of local circulation in a wide, stratified fjord including exchange of water with the adjacent ocean, due to constant upfjord wind. *In:* Skjoldal, H.R., Hopkins, C., Erikstad, K. E. & Leinaas, H. P. (eds) *Ecology of Fjords and Coastal Waters* Elsevier Science B.V., Amsterdam, The Netherlands. 177-184.

Bergh, J. 2004. Measured and modelled tidally driven mean circulation under ice cover in Van Mijenfjorden. M.Sc. Thesis, Göteborg University, Göteborg.

Cottier, F. Nilsen, F., Skogseth, R., Tverberg, V., Svendsen, H. & Skarðhamar, J. 2010. Arctic fjords: A review of the oceanographic environment and dominant physical processes. (This book)

Cottier, F., Tverberg, V., Inall, M., Svendsen, H., Nilsen, F. & Griffiths, C. 2005. Water mass modification in an Arctic fjord through cross-shelf exchange: The seasonal hydrography of Kongsfjorden, Svalbard. *Journal of Geophysical Research* **110**, C12005, doi:10.1029/2004JC002757.

Cushman-Roisin, B., Asplin, L. & Svendsen, H. 1994. Upwelling in broad fjords. *Continental Shelf Research* **14 (15)**, 1701-1721.

Emery, W. J. & Thomson, R. E. 1997. *Data analysis methods in physical oceanography, second and revised edition*. Elsevier Science B.V., Amsterdam, The Netherlands.

Farmer, D. M. & Freeland, H. J. 1983. The physical oceanography of fjords. *Progress in Oceanography* **12**, 147-220.

Fer, I. & Widell, K. 2007. Early spring turbulent mixing in an ice-covered Arctic fjord during transition to melting. *Continental Shelf Research* **27**, 1980-1999.

Hald, M., Dahlgren, T., Olsen, T. E. & Lebesbye, E. 2001. Late Holocene palaeoceanography in Van Mijenfjorden, Svalbard. *Polar Research* **20 (1),** 23-35.

Hanssen-Bauer, I., Solås, M. K. & Steffensen, E. L. 1990. *The climate of Spitsbergen. DNMI rapport nr. 39/90.* The Norwegian meteorological institute, Oslo.

Inall, M. E., Rippeth, T. P., Griffiths, C. R. & Wiles, P. 2005. Evolution and distribution of TKE production and dissipation within a stratified flow over topography. *Geophysical Research Letters* **32**, doi: 10.1029/2004GL022289.

Ingvaldsen, R., Reitan, M. B., Svendsen, H. & Asplin, L. 2001. The upper layer circulation in Kongsfjorden and Krossfjorden - a complex fjord system on the west coast of Spitsbergen. *Polar Research Special Issue* **54,** 393-407.

Nilsen, F., Cottier, F., Skogseth, R. & Mattsson, S. 2008. Fjord-shelf exchanges controlled by ice and brine production: The interannual variation of Atlantic Water in Isfjorden, Svalbard. *Continental Shelf Research* **28**, 1838-1853.

Norwegian hydrographic service 1990. *Arctic pilot, sailing directions travellers' guide, Svalbard and Jan Mayen, volume 7, 2 edition*. Stavanger, Norway: The Norwegian Hydrographic Service and Norwegian Polar Institute.

Rowan D.E., Péwé T.L., Péwé R.H. & Stuckenrath R. 1982. Holocene glacial geology of the Svea lowland, Spitsbergen, Svalbard. *Geografiska annaler* **64 A (1-2)**, 35-51.

Schei, B., Eilertsen, H. C., Falk-Petersen, S., Gulliksen, B. & Taasen, J. P. 1979. Marinbiologiske undersøkelser i Van Mijenfjorden (Vest-Spitsbergen) etter en oljelekkasje ved Seagruva 1978 . *TROMURA, Naturvitenskap nr. 2*. Universitetet i Tromsø, Institutt for museumsvirksomhet, Tromsø, Norway.

Stigebrandt, A. 1980. Some aspects of tidal interaction with fjord constrictions. *Estuarine Coastal and marine Science* **11**, 151-166.

Støylen, E. & Weber, J. E. Mass transport induced by internal Kelvin waves beneath shore fast ice. Accepted for publication in *Journal of Geophysical Research*.

Svendsen, H. 1986. Mixing and exchange processes in estuaries, fjords and shelf waters. *In*: Skreslet, S. (ed.): *The role of freshwater outflow in coastal marine ecosystems*. *NATO ASI Series G7*, 13-45.

Svendsen, H. 1995. Physical oceanography of coupled fjord-coast systems in northern Norway with special focus on frontal dynamics and tides. *In:* Skjoldal, H.R., Hopkins, C., Erikstad, K. E. & Leinaas, H. P. (eds) *Ecology of Fjords and Coastal Waters* Elsevier Science B.V., Amsterdam, The Netherlands. 149-164.

Svendsen, H., Beszczynska-Møller, A., Hagen, J. O., Lefauconnier, B., Tverberg, V., Gerland, S., Ørbæk, J. B., Bischof, K., Papucci, C., Zajaczkowski, M., Azzolini, R., Bruland, O., Wiencke, C., Winter, J.-G. & Dallmann, W. 2002. The physical environment of Kongsfjorden-Krossfjorden, an Arctic fjord system in Svalbard. *Polar Research* **21 (1)**, 133-166.

Tverberg, V. & Nøst, O. A. 2009. Eddy overturning across a shelf edge front: Kongsfjorden, west Spitsbergen. *Journal of Geophysical Research* **114**, C04024, doi:10.1029/2008JC005106.

Weslawski, J. M., Koszteyn, J., Kwasniewski, S., Swerper, S. & Ryg, M. 1991. Summer hydrology and zooplankton in two Svalbard fjords. *Polish polar research* **12**, 445-460.

Widell, K., Fer, I. & Haugan, P. M. 2006. Salt release from warming sea ice. *Geophysical Research Letters* **33**, L12501, doi:10.1029/2006GL026262.

Table 1. *Positions and measuring depth of the current meter moorings in Van Mijenfjorden 28 July – 3 August 1996*

Mooring	Position	Measuring depths
Innermost	77°48.00 N, 15°56.4 E	2, 30 and 60 m
Northern	77°48.46 N, 15°15.02 E	2, 10, 30 and 70 m
Southern	77°46.11 N, 15°25.38 E	2, 10, 30 and 70 m

Table 2. *12-hour mean wind speed and direction for the three periods of CTD surveys*

Survey	Time	Wind speed (m s^{-1})	Wind direction
1	27/7 22:00 – 28/7 10:00	0.93	264
2	31/7 03:00 – 15:00	6.81	294
3	1/8 17:00 – 2/8 05:00	1.10	293

Figure captions

Figure 1: Map of Van Mijenfjorden with depth contours (m), and positions for CTD stations (circles), time series station (star) and current meter moorings (squares).

Figure 2: Vertical along-fjord sections of salinity (a) and temperature (b) distributions from the first (upper panels), second (middle panels) and third (lower panels) surveys. Seen from south, i.e. west is to the left in the figures.

Figure 3: Vertical profiles of salinity (left) and temperature (right) in the inner part of the fjord (upper panels) and northern side of the outer part of the fjord (lower panels) from the first (solid line), second (broken line) and third (dotted line) surveys.

Figure 4: Distribution of salinity (upper panels) and temperature (lower panels) along a cross-section of the fjord, as measured during the first (left panels) and second (right panels) surveys. Seen from west, i.e. north is to the left in the figures.

Figure 5: Hourly development of the depth of the salinity 33 isoline at the time-series station.

Figure 6: Measurements of (a) wind and currents at the innermost mooring, and current measurements from the moorings on the (b) northern and (c) southern side of the outer basin. Note that the vertical figure axis is directed east – west, and that all vectors represent the direction towards which the currents and winds are moving.

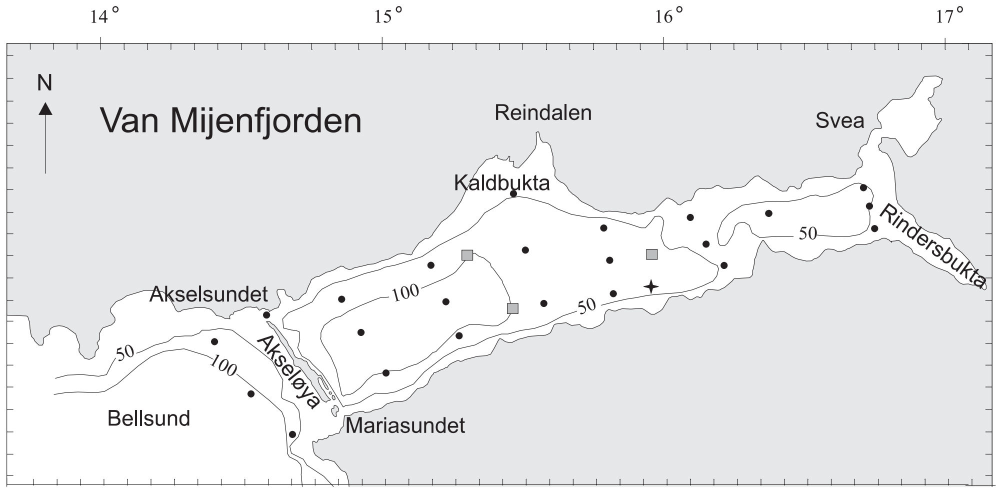
14°
15°
16°
17°
N
Van Mijenfjorden
Reindalen
Svea
Kaldbukta
77°55
77°50
Rindersbukta
50
Akselsundet
100
50
77°45
50
Akseløya
100
Bellsund
Mariasundet
77°40

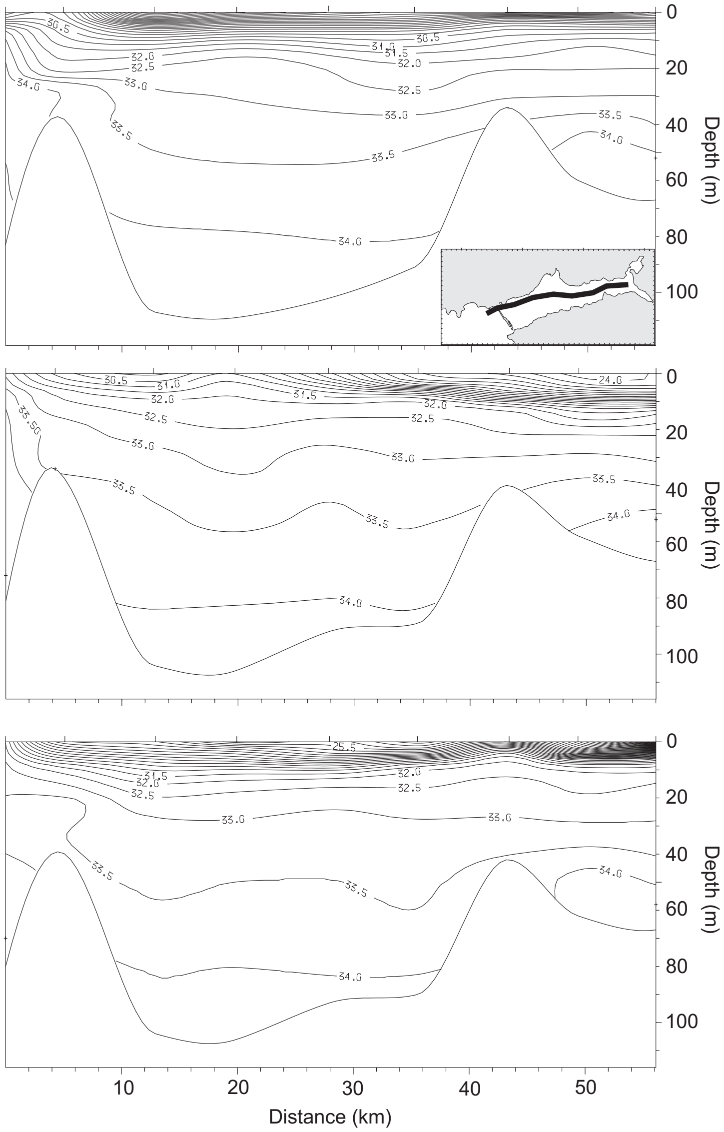
30.5
31.0
31.5
32.0
32.5
33.0
33.5
34.0
33.50
24.0
25.5
Depth (m)
0
20
40
60
80
100
10
20
30
40
50
Distance (km)

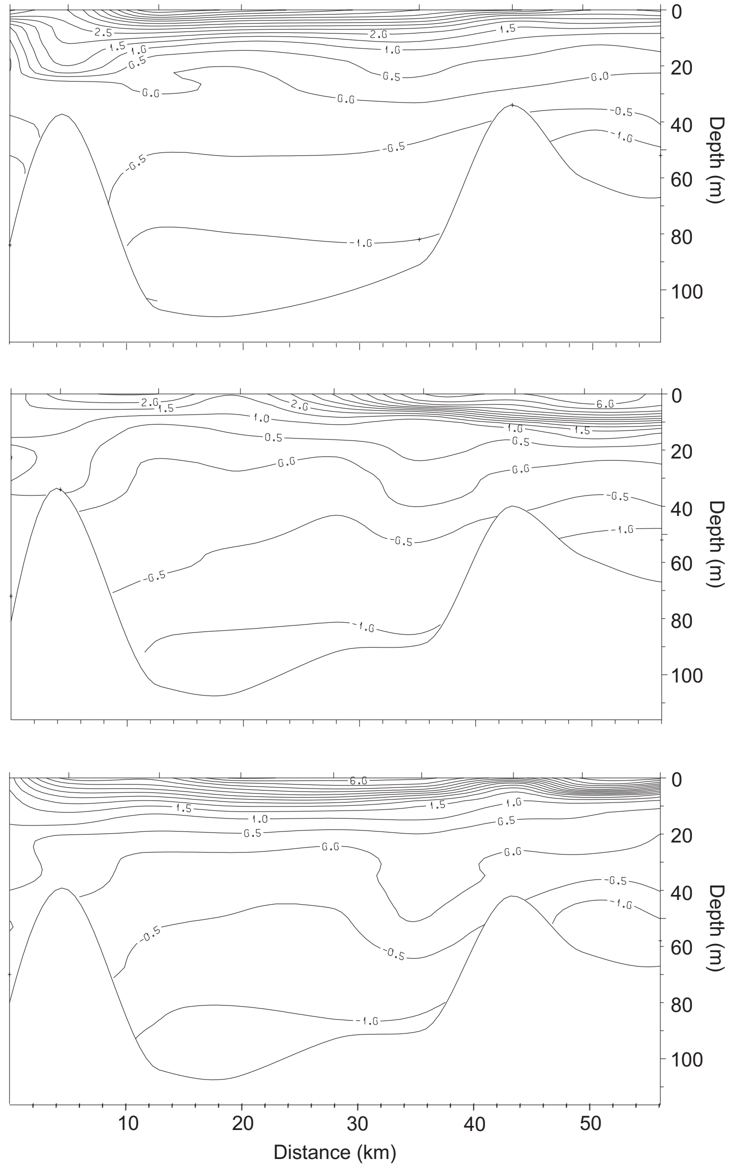2.5
2.0
1.5
1.0
0.5
0.0
-0.5
-1.0
0.0
-0.5
-1.0
0
20
40
60
80
100
Depth (m)
2.0
1.5
1.0
0.5
0.0
2.0
1.0
1.5
0.5
0.0
-0.5
-1.0
-0.5
-1.0
0
20
40
60
80
100
Depth (m)
0.0
1.5
1.0
0.5
0.0
1.5
1.0
0.5
0.0
-0.5
-1.0
-0.5
-1.0
0
20
40
60
80
100
Depth (m)
10
20
30
40
50
Distance (km)

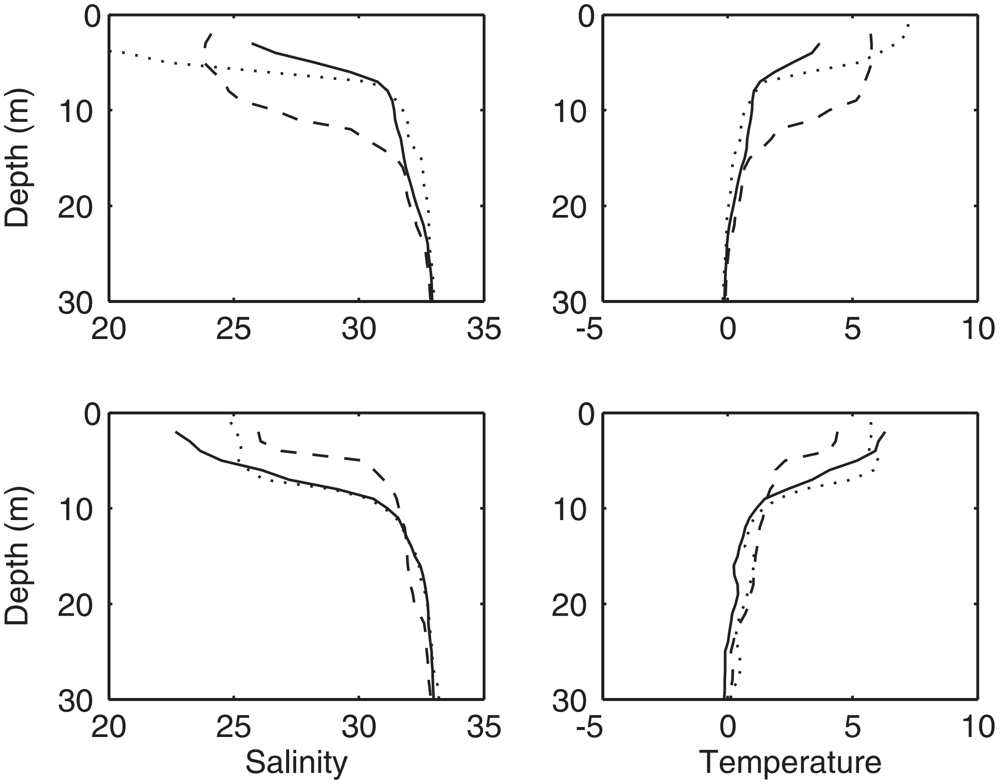
0
10
20
30
Depth (m)
20
25
30
35
Salinity
-5
0
5
10
Temperature

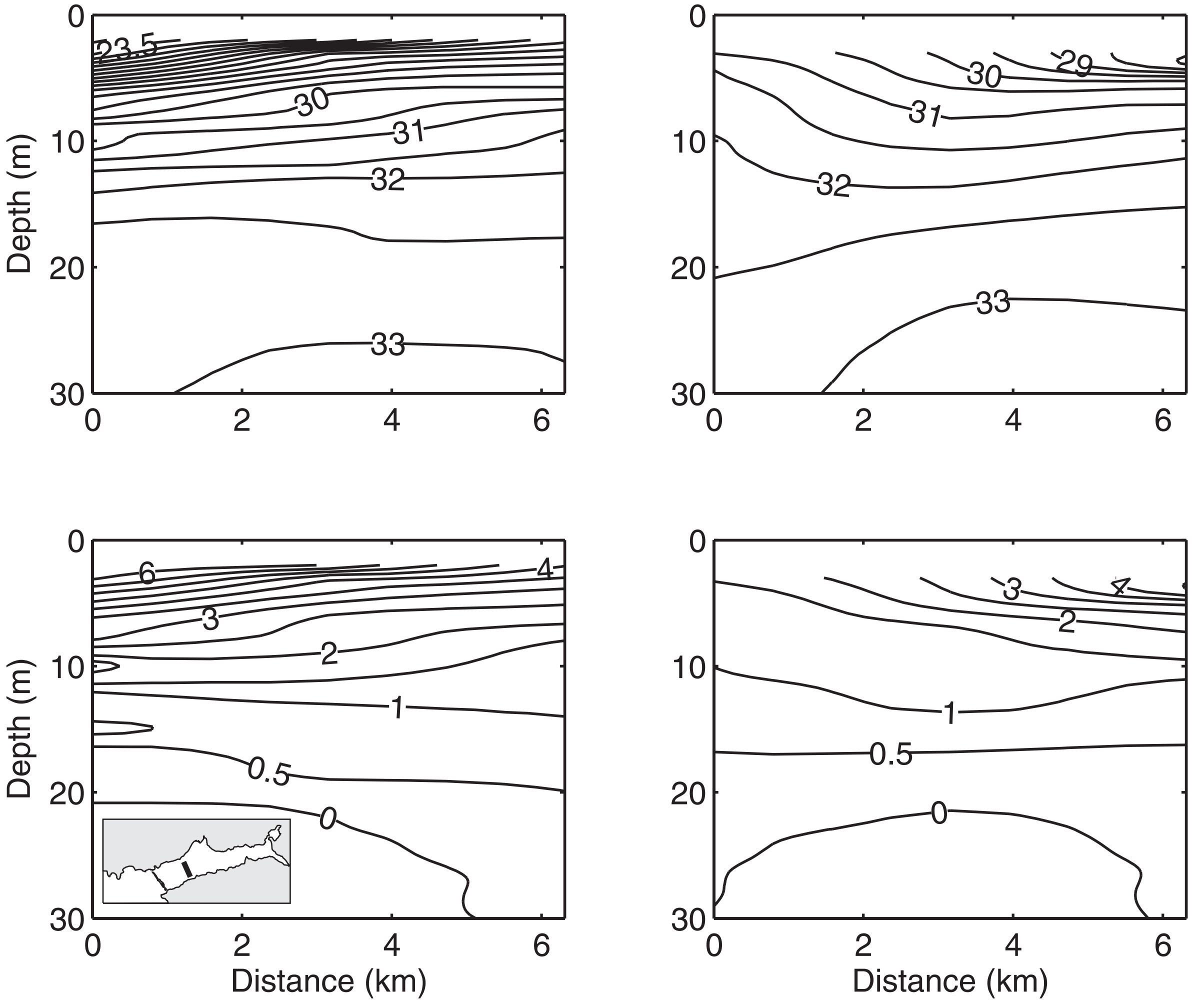

Depth (m)
0
10
20
30
23.5
30
31
32
33
29
0
2
4
6
6
4
3
2
1
0.5
0
Distance (km)

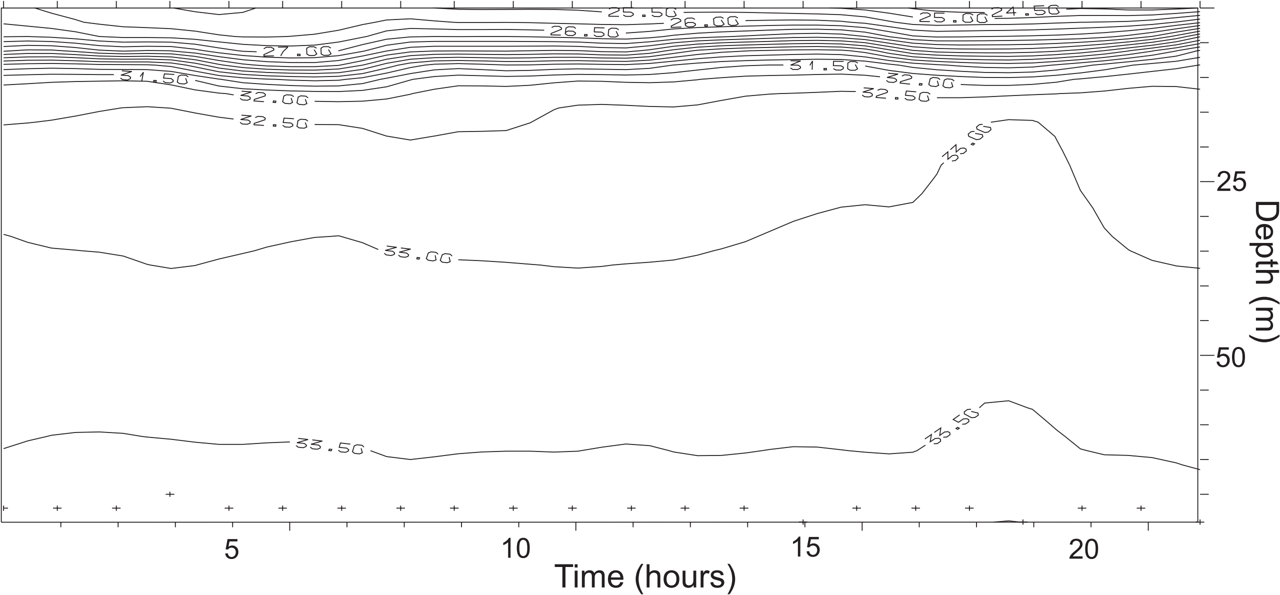
25.50
26.00
24.50
25.00
26.50
27.00
31.50
31.50
32.00
32.00
32.50
32.50
33.00
33.00
33.50
33.50
25
50
Depth (m)
5
10
15
20
Time (hours)

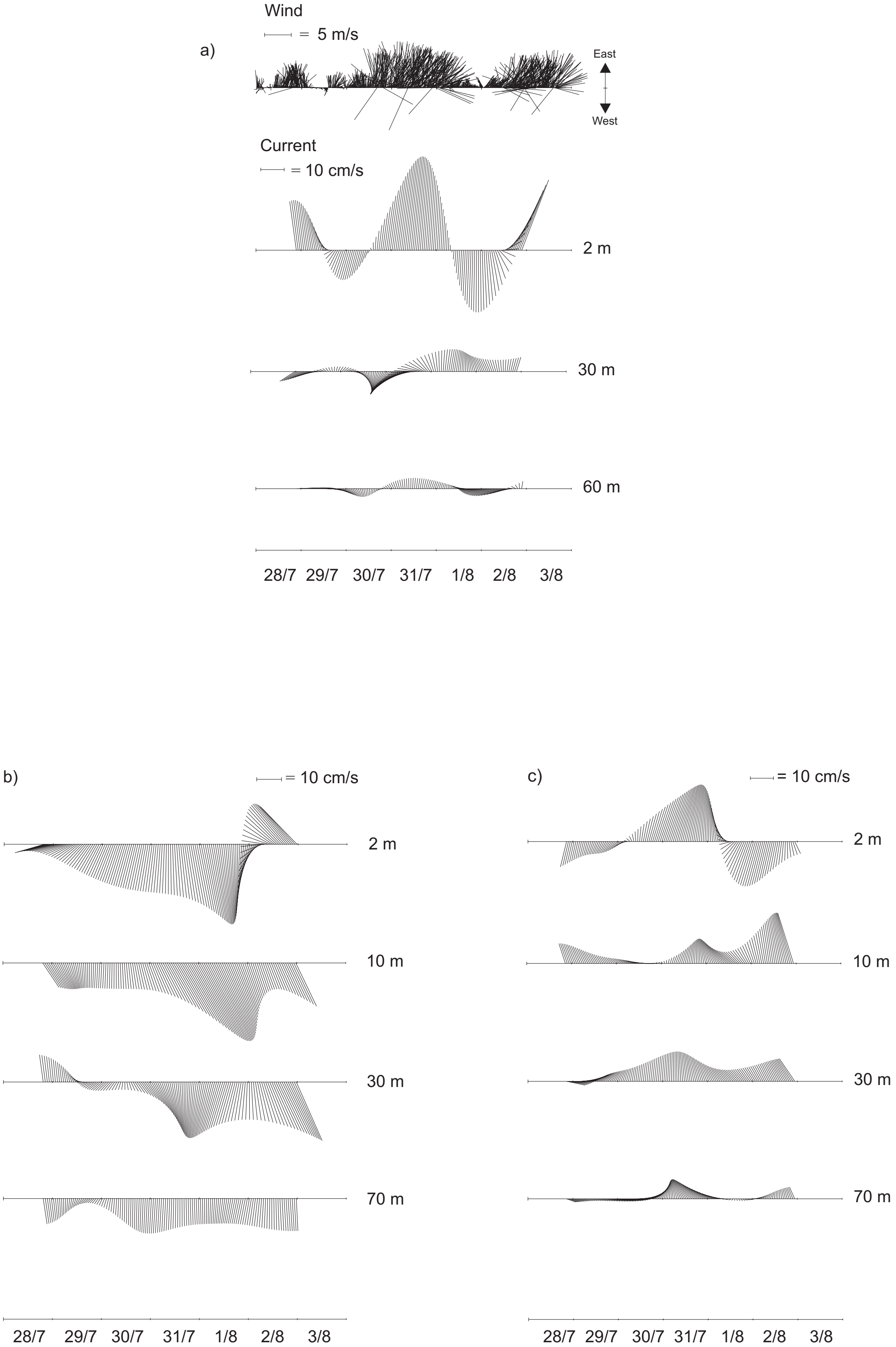
a)
Wind
= 5 m/s
East
West
Current
= 10 cm/s
2 m
30 m
60 m
28/7
29/7
30/7
31/7
1/8
2/8
3/8
b)
= 10 cm/s
2 m
10 m
30 m
70 m
28/7
29/7
30/7
31/7
1/8
2/8
3/8
c)
= 10 cm/s
2 m
10 m
30 m
70 m
28/7
29/7
30/7
31/7
1/8
2/8
3/8